IFS of a high metallicity GEHR in NGC6946

Rubén García-Benito & Ángeles Díaz

Universidad Autónoma de Madrid

Liu Xiaowei
(KAVLI Institute at Beijing University)

VII Workshop
Estallidos de formación estelar

Outline

1. Introduction
   - The Galaxy: NGC 6946
   - The region(s)
2. Observations & Data Reduction
   - Observations
   - Reduction
3. Analysis
   - Fit population
   - Maps
4. Conclusions



The Galaxy: NGC 6946



NGC 6946: Fireworks Galaxy

- Prolific producer of SNe in the last century
- Largest number of SN events ever recorded

Properties

The Galaxy: NGC 6946



NGC 6946: Fireworks Galaxy

- Prolific producer of SNe in the last century
- Largest number of SN events ever recorded

Properties

The Galaxy: NGC 6946



NGC 6946: Fireworks Galaxy

- Prolific producer of SNe in the last century
- Largest number of SN events ever recorded

Properties

Size	11.5 × 9.8 arcmin

The Galaxy: NGC 6946



NGC 6946: Fireworks Galaxy

- Prolific producer of SNe in the last century
- Largest number of SN events ever recorded

Properties

Size	11.5 × 9.8 arcmin
Distance	5.9 Mpc (v_0 = 46km s^{-1})
Scale	28.6 pc/"

The Galaxy: NGC 6946



NGC 6946: Fireworks Galaxy

- Prolific producer of SNe in the last century
- Largest number of SN events ever recorded

Properties

Size	11.5×9.8 arcmin
Distance	5.9 Mpc ($v_h = 46 \mathrm{km\ s^{-1}}$)
Scale	28.6 pc/″
Radius	$R_{eff} = 6.23$ kpc / $R_{25} = 9.8$kpc



The Galaxy: NGC 6946



NGC 6946: Fireworks Galaxy

- Prolific producer of SNe in the last century
- Largest number of SN events ever recorded

Properties

Size	11.5×9.8 arcmin
Distance	5.9 Mpc ($v_h = 46 \mathrm{km\ s^{-1}}$)
Scale	28.6 pc/″
Radius	$R_{eff} = 6.23$ kpc / $R_{25} = 9.8$kpc

The Galaxy: NGC 6946



NGC 6946: Fireworks Galaxy

- Prolific producer of SNe in the last century
- Largest number of SN events ever recorded

Properties

Size	11.5×9.8 arcmin
Distance	5.9 Mpc ($v_h = 46 \mathrm{km\ s^{-1}}$)
Scale	28.6 pc/″
Radius	$R_{eff} = 6.23$ kpc / $R_{25} = 9.8$kpc

Outer Galaxy HII Region Abundances in NGC 6946

Belley & Roy (1992) + Roy Belley (1993)

- Narrow-band images of Hα, Hβ, 6584 [NII], 5007 [OIII]
- Empirically derived O/H abundances for over 100 HII regions
- O/H gradient = -0.089 $\pm$ 0.003 dex/kpc, central abundance of 12+log(O/H) = 9.31 $\pm$ 0.02



Outer Galaxy HII Region Abundances in NGC 6946

Belley & Roy (1992) + Roy Belley (1993)

- Narrow-band images of Hα, Hβ, 6584 [NII], 5007 [OIII]
- Empirically derived O/H abundances for over 100 HII regions
- O/H gradient = -0.089 $\pm$ 0.003 dex/kpc, central abundance of 12+log(O/H) = 9.36 $\pm$ 0.02



Outer Galaxy HII Region Abundances in NGC 6946

Belley & Roy (1992) + Roy Belley (1993)

- Narrow-band images of Hα, Hβ, 6584 [NII], 5007 [OIII]
- Empirically derived O/H abundances for over 100 HII regions
- O/H gradient = -0.089 $\pm$ 0.003 dex/kpc, central abundance of 12+log(O/H) = 9.36 $\pm$ 0.02



Outer Galaxy HII Region Abundances in NGC 6946

Belley & Roy (1992) + Roy Belley (1993)

- Narrow-band images of Hα, Hβ, 6584 [NII], 5007 [OIII]
- Empirically derived O/H abundances for over 100 HII regions
- O/H gradient = -0.089 $\pm$ 0.003 dex/kpc, central abundance of 12+log(O/H) = 9.36 $\pm$ 0.02



Outer Galaxy HII Region Abundances in NGC 6946

Belley & Roy (1992) + Roy Belley (1993)

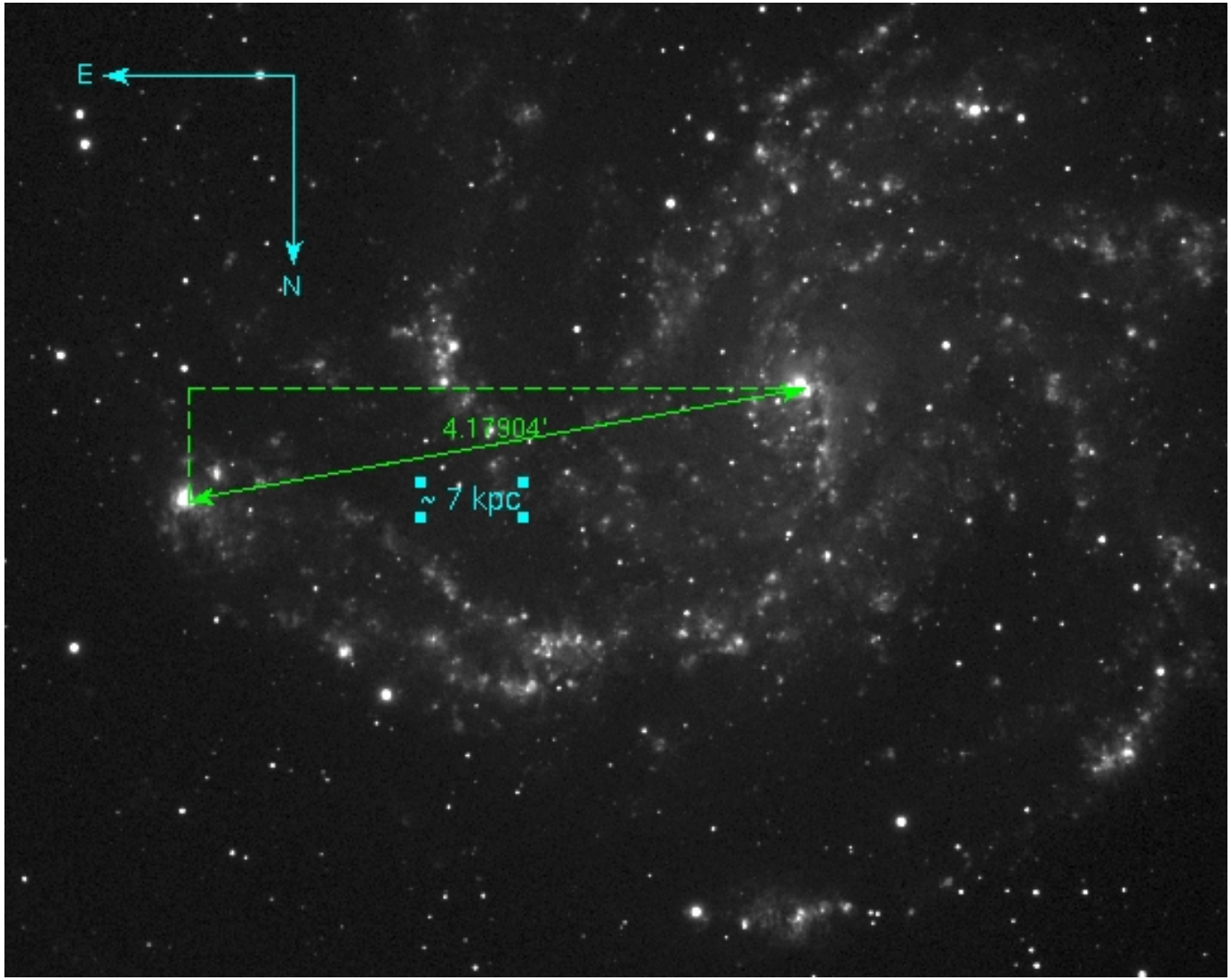
- Narrow-band images of Hα, Hβ, 6584 [NII], 5007 [OIII]
- Empirically derived O/H abundances for over 100 HII regions
- O/H gradient = -0.089 $\pm$ 0.003 dex/kpc, central abundance of 12+log(O/H) = 9.36 $\pm$ 0.02



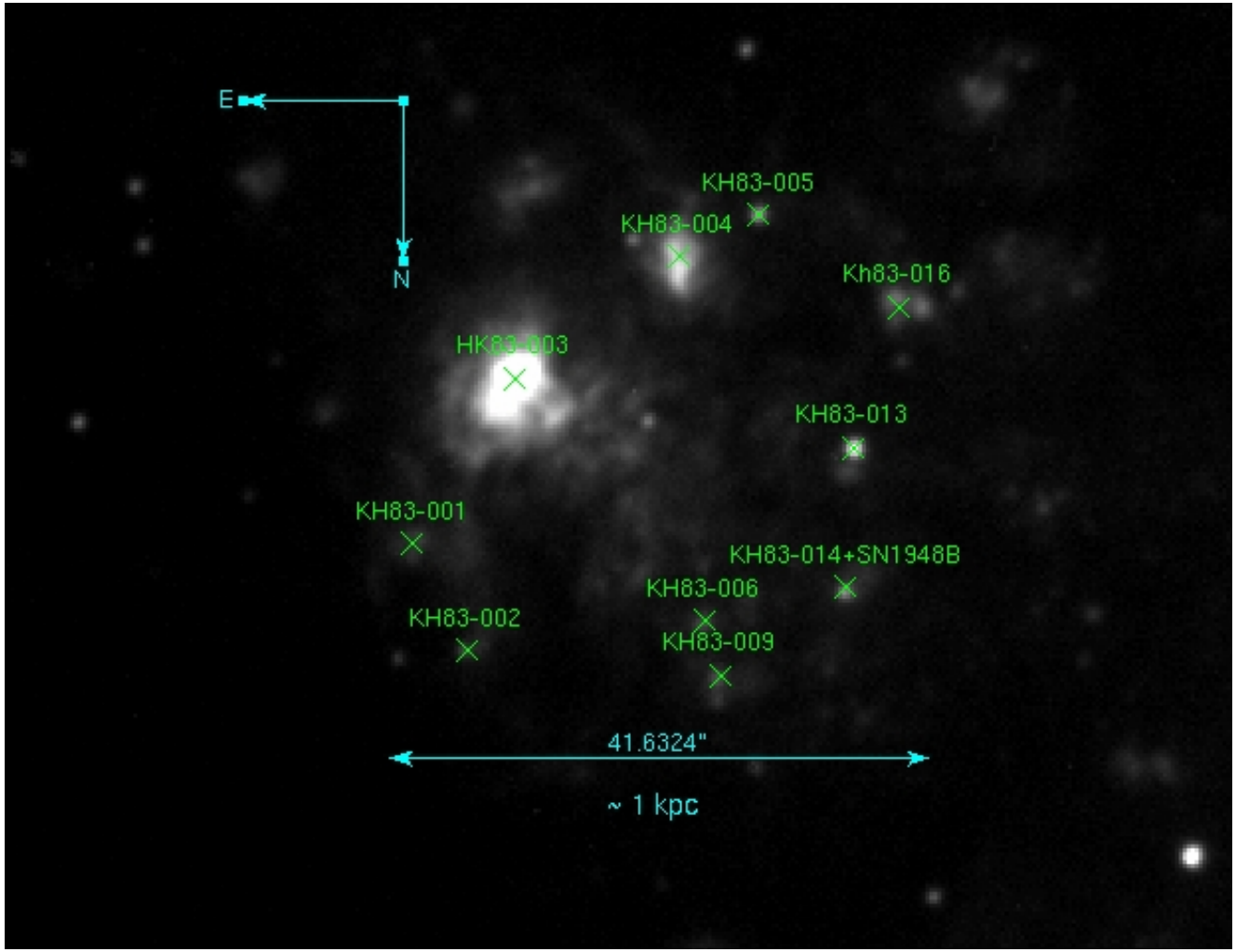
Outer Galaxy HII Region Abundances in NGC 6946



The region(s): where is it?



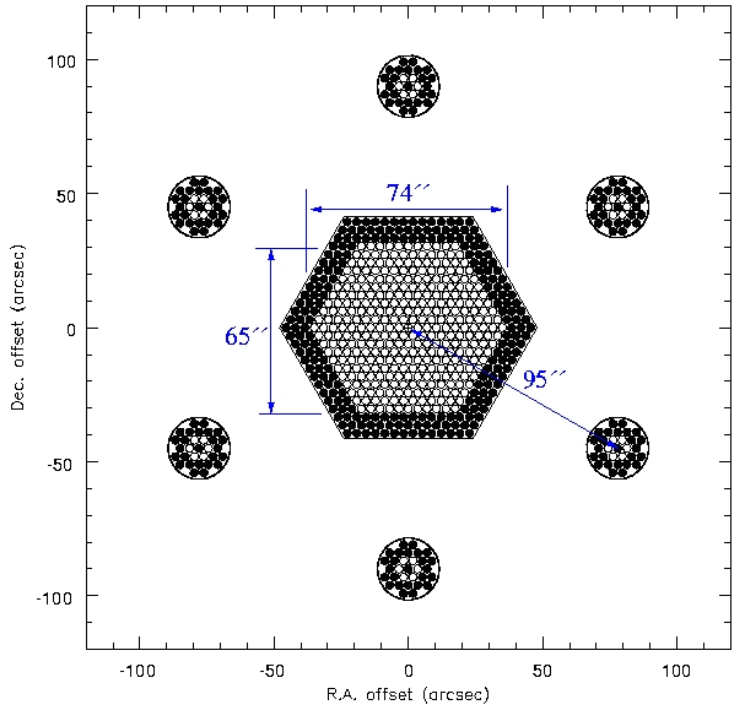
Hα morphology



Observatory:KPNO • Year: 2001 • Observers: Calzetti & Dale

Telescope and detector

- Calar Alto Observatory 3.5m Telescope
- PMAS spectrograph (IFU) PPAK mode
- 382 fibers = 15 calibration + 36 sky + 331 science
- fiber = 2.7″diameter
- Hexagonal field-of-view of 72″× 64″
- Filling factor of ∼ 65 %
- Sky fibers in a circular distribution at ∼ 90″



Observations

Observers: A. Díaz, G. Hägele & J. López

Pointing	Exptime (s)	Grating	Spec. Range (Å)	Dispersion (Å/pix)	Date
NGC 6946	3×500	V300	3700-7000	3.2	09/07/2008
BD+28D4211	3×30	V300	3700-7000	3.2	09/07/2008
NGC 6946	3×500	V300	7000-10100	3.2	09/08/2008
BD+17D4708	3×30	V300	7000-10100	3.2	09/09/2008



Reduction

Packages

R3D (Sánchez 2006), E3D (Sánchez 2004), IRAF & Python

Main reductions steps:

- Master bias averagin all bias frames
- Location spectra in CCD using a continuum illuminated exposure



Reduction

Packages

R3D (Sánchez 2006), E3D (Sánchez 2004), IRAF & Python

Main reductions steps:

- Master bias averagin all bias frames
- Location spectra in CCD using a continuum illuminated exposure



Reduction

Packages

R3D (Sánchez 2006), E3D (Sánchez 2004), IRAF & Python

Main reductions steps:

- Master bias averagin all bias frames
- Location spectra in CCD using a continuum illuminated exposure



Reduction

- Each spectrum extracted by simple gaussian extraction along the cross-dispersion (vs coadding flux within an aperture of 5 pixels)
- Blue wavelength calibration using an HeHgCs + ThAr lamp
- Red wavelenght calibration using sky lines (HeHgCs + ThAr has not bright lines $\rightarrow$ better with sky)
- Distortion corrected using ThAr through the calibration fibers
- Fiber-to-fiber transmission corrected comparing science frames with the corresponding continuum illuminated ones
- Average background spectrum from 36 fibers for sky subtraction



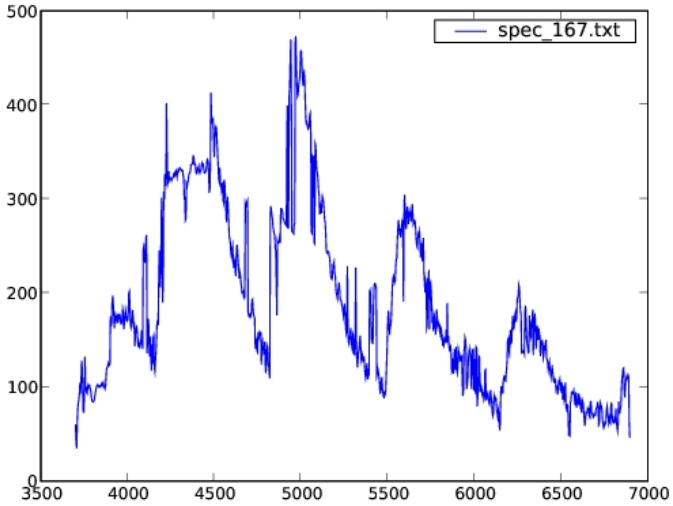
Reduction

- Each spectrum extracted by simple gaussian extraction along the cross-dispersion (vs coadding flux within an aperture of 5 pixels)
- Blue wavelength calibration using an HeHgCs + ThAr lamp
- Red wavelenght calibration using sky lines (HeHgCs + ThAr has not bright lines $\rightarrow$ better with sky)
- Distortion corrected using ThAr through the calibration fibers
- Fiber-to-fiber transmission corrected comparing science frames with the corresponding continuum illuminated ones
- Average background spectrum from 36 fibers for sky subtraction



Reduction

- Each spectrum extracted by simple gaussian extraction along the cross-dispersion (vs coadding flux within an aperture of 5 pixels)
- Blue wavelength calibration using an HeHgCs + ThAr lamp
- Red wavelenght calibration using sky lines (HeHgCs + ThAr has not bright lines $\longrightarrow$ better with sky)
- Distortion corrected using ThAr through the calibration fibers
- Fiber-to-fiber transmission corrected comparing science frames with the corresponding continuum illuminated ones
- Average background spectrum from 36 fibers for sky subtraction



Reduction

- Each spectrum extracted by simple gaussian extraction along the cross-dispersion (vs coadding flux within an aperture of 5 pixels)
- Blue wavelength calibration using an HeHgCs + ThAr lamp
- Red wavelenght calibration using sky lines (HeHgCs + ThAr has not bright lines $\longrightarrow$ better with sky)
- Distortion corrected using ThAr through the calibration fibers
- Fiber-to-fiber transmission corrected comparing science frames with the corresponding continuum illuminated ones
- Average background spectrum from 36 fibers for sky subtraction



Reduction

- Each spectrum extracted by simple gaussian extraction along the cross-dispersion (vs coadding flux within an aperture of 5 pixels)
- Blue wavelength calibration using an HeHgCs + ThAr lamp
- Red wavelenght calibration using sky lines (HeHgCs + ThAr has not bright lines $\rightarrow$ better with sky)
- Distortion corrected using ThAr through the calibration fibers
- Fiber-to-fiber transmission corrected comparing science frames with the corresponding continuum illuminated ones
- Average background spectrum from 36 fibers for sky subtraction



Reduction

- Each spectrum extracted by simple gaussian extraction along the cross-dispersion (vs coadding flux within an aperture of 5 pixels)
- Blue wavelength calibration using an HeHgCs + ThAr lamp
- Red wavelenght calibration using sky lines (HeHgCs + ThAr has not bright lines $\rightarrow$ better with sky)
- Distortion corrected using ThAr through the calibration fibers
- Fiber-to-fiber transmission corrected comparing science frames with the corresponding continuum illuminated ones
- Average background spectrum from 36 fibers for sky subtraction



Reduction

- Each spectrum extracted by simple gaussian extraction along the cross-dispersion (vs coadding flux within an aperture of 5 pixels)
- Blue wavelength calibration using an HeHgCs + ThAr lamp
- Red wavelenght calibration using sky lines (HeHgCs + ThAr has not bright lines $\rightarrow$ better with sky)
- Distortion corrected using ThAr through the calibration fibers
- Fiber-to-fiber transmission corrected comparing science frames with the corresponding continuum illuminated ones
- Average background spectrum from 36 fibers for sky subtraction



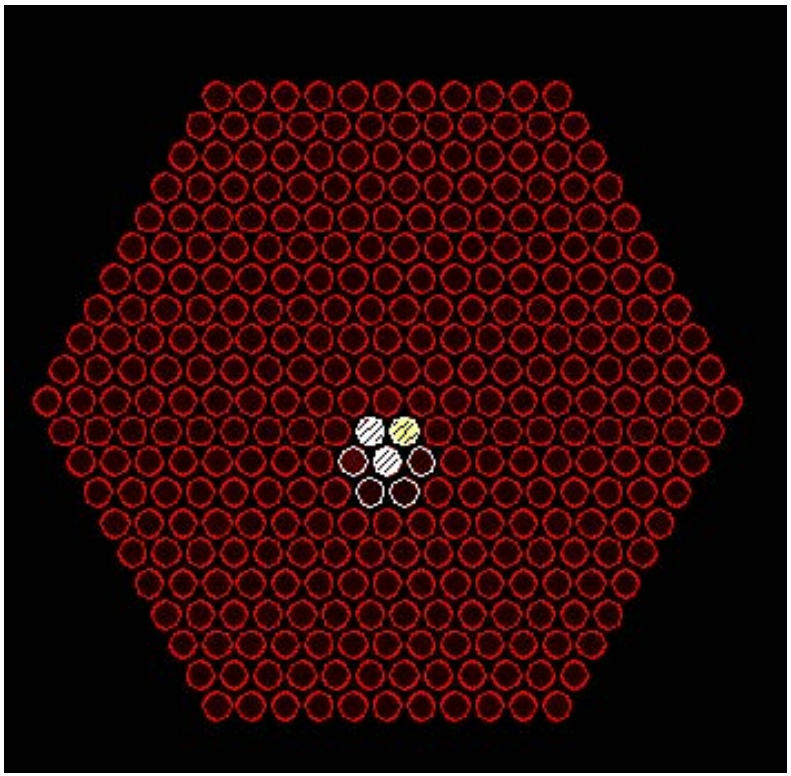
Reduction

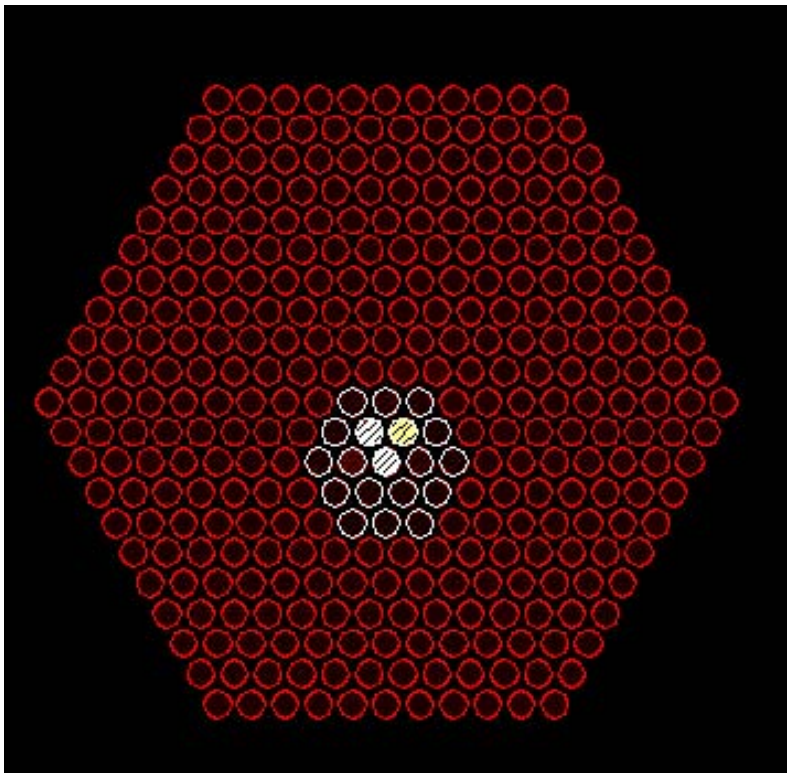
- Each spectrum extracted by simple gaussian extraction along the cross-dispersion (vs coadding flux within an aperture of 5 pixels)
- Blue wavelength calibration using an HeHgCs + ThAr lamp
- Red wavelenght calibration using sky lines (HeHgCs + ThAr has not bright lines $\rightarrow$ better with sky)
- Distortion corrected using ThAr through the calibration fibers
- Fiber-to-fiber transmission corrected comparing science frames with the corresponding continuum illuminated ones
- Average background spectrum from 36 fibers for sky subtraction



Flux calibration: standard star

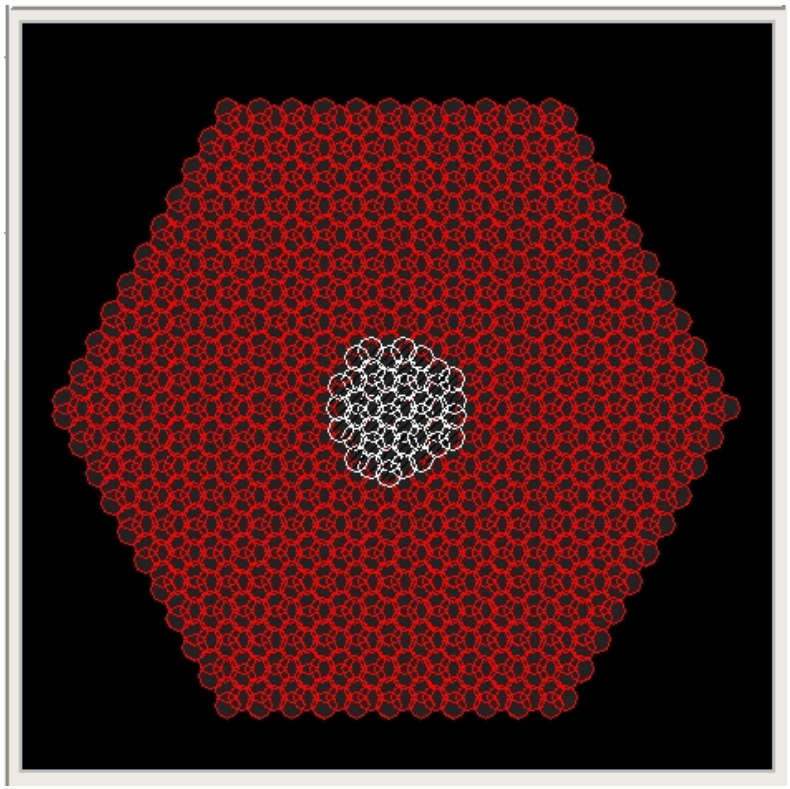
No dithering

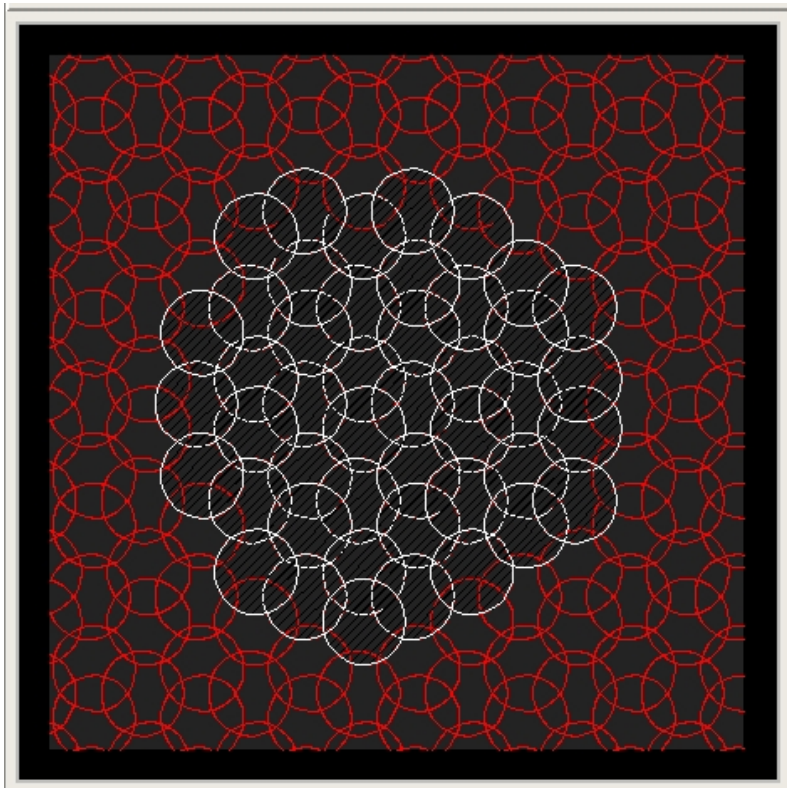




Flux calibration: standard star

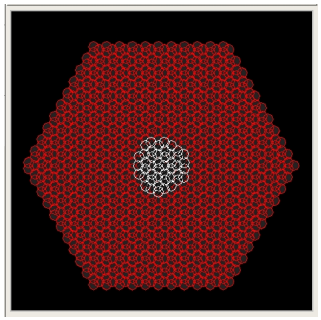
Dithering

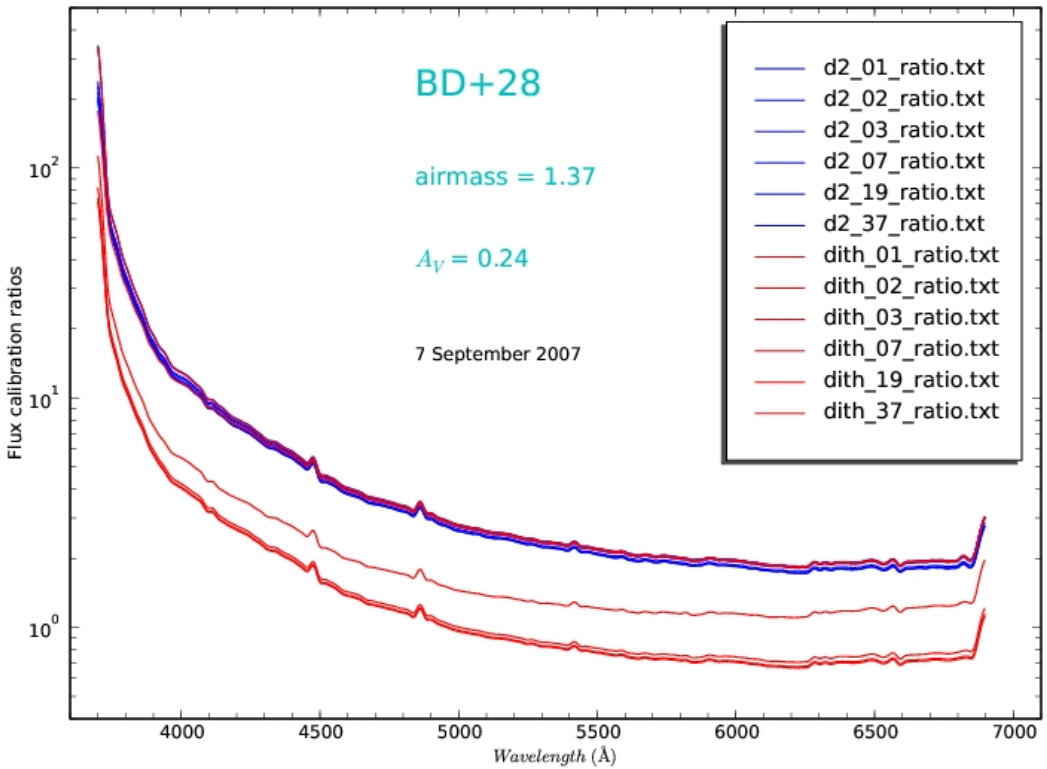




Flux calibration: standard star

Dithering

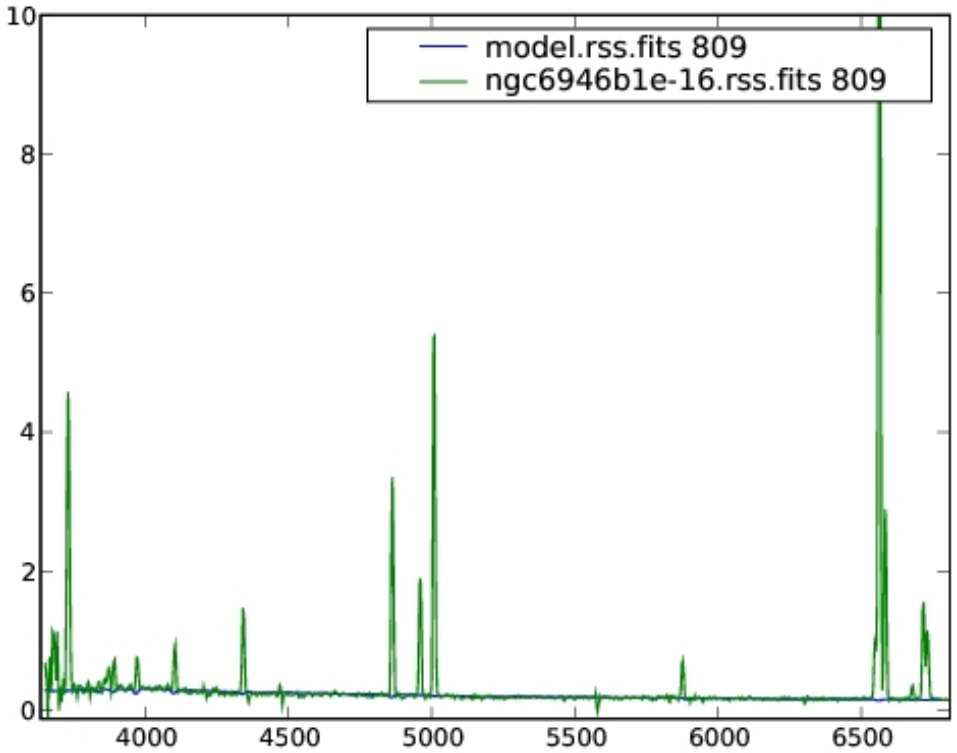




Fit continuum

FIT3D (Sánchez et al. 2007)

Fitting tool to fit emission lines and continuum spectrum.

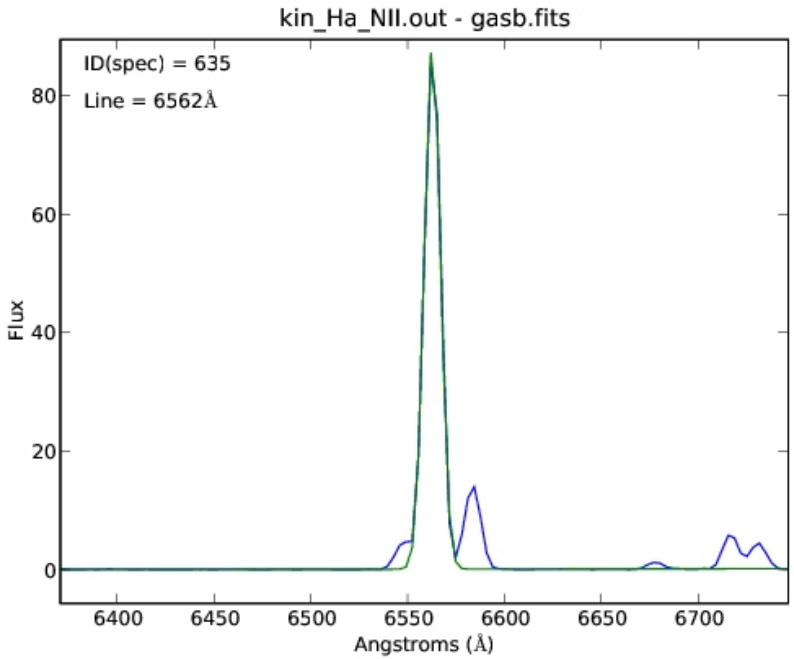


Bases: $Z = Z_{\odot}$ from 5 Myr up to 900 Myr $\leftrightarrow$ Result = GAS RSS SPECTRA

Fitting lines

- Single Gaussian to each emission line
- Polynomial function to characterize continuum (low order)
- Definition of emission line systems (kinematically coupled) for debleding lines

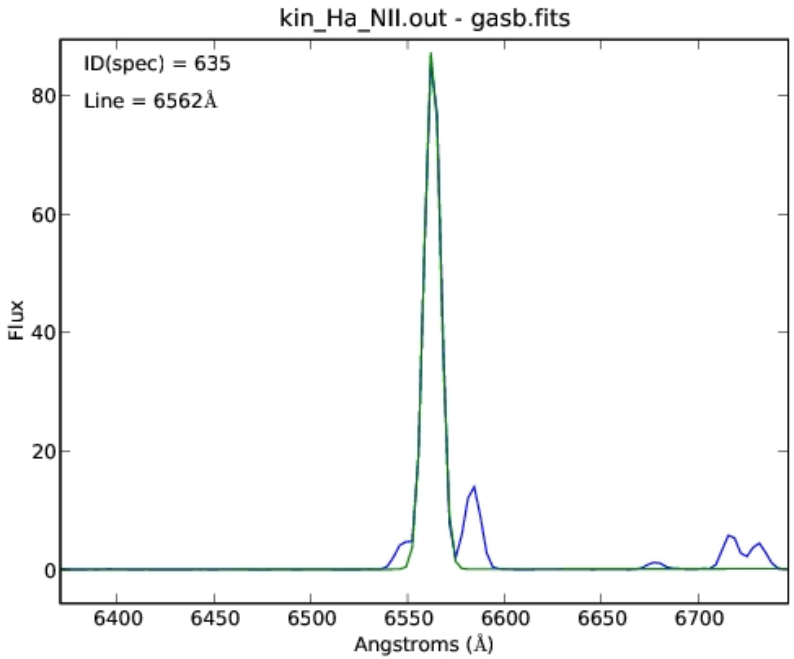
Similar results as combined Python + IRAF fitting tools



Fitting lines

- Single Gaussian to each emission line
- Polynomial function to characterize continuum (low order)
- Definition of emission line systems (kinematically coupled) for debleding lines

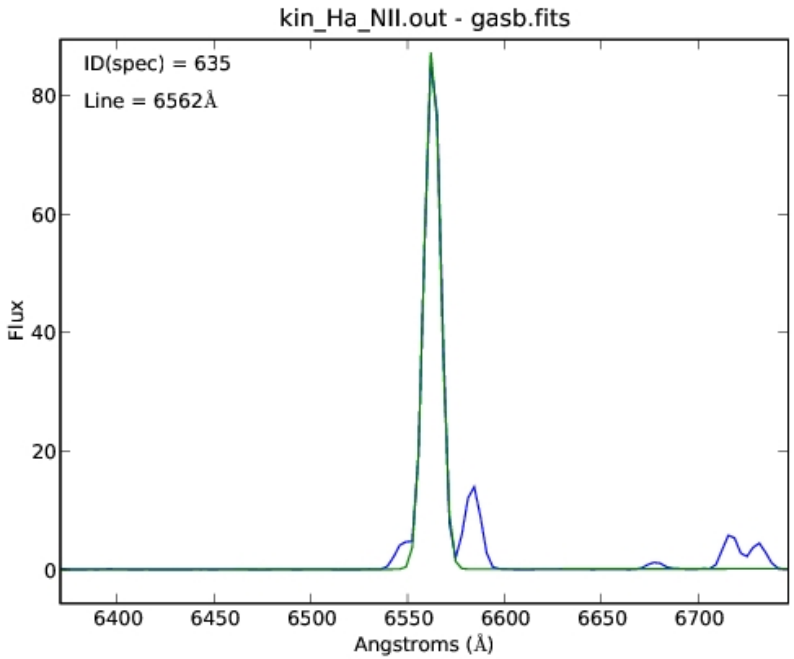
Similar results as combined Python + IRAF fitting tools



Fitting lines

- Single Gaussian to each emission line
- Polynomial function to characterize continuum (low order)
- Definition of emission line systems (kinematically coupled) for debleding lines

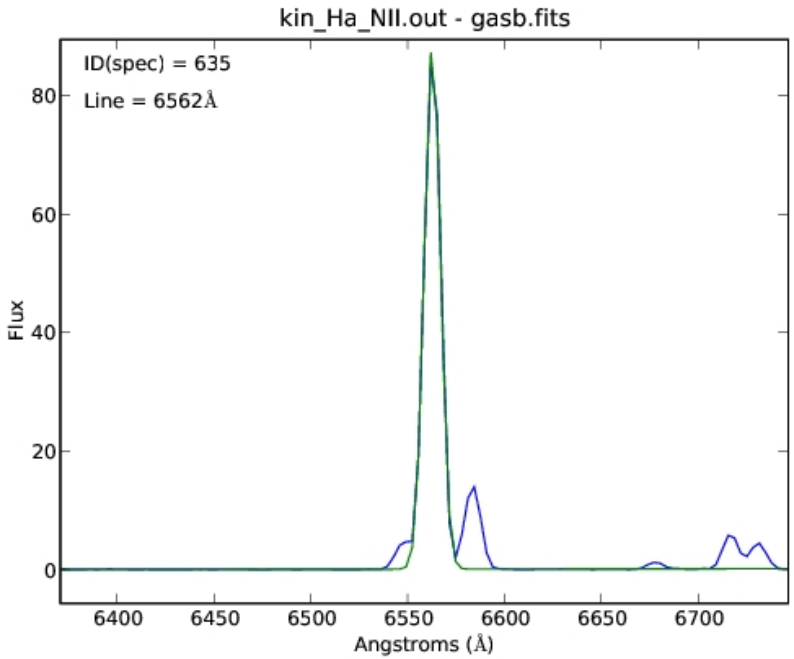
Similar results as combined Python + IRAF fitting tools



Fitting lines

- Single Gaussian to each emission line
- Polynomial function to characterize continuum (low order)
- Definition of emission line systems (kinematically coupled) for debleding lines

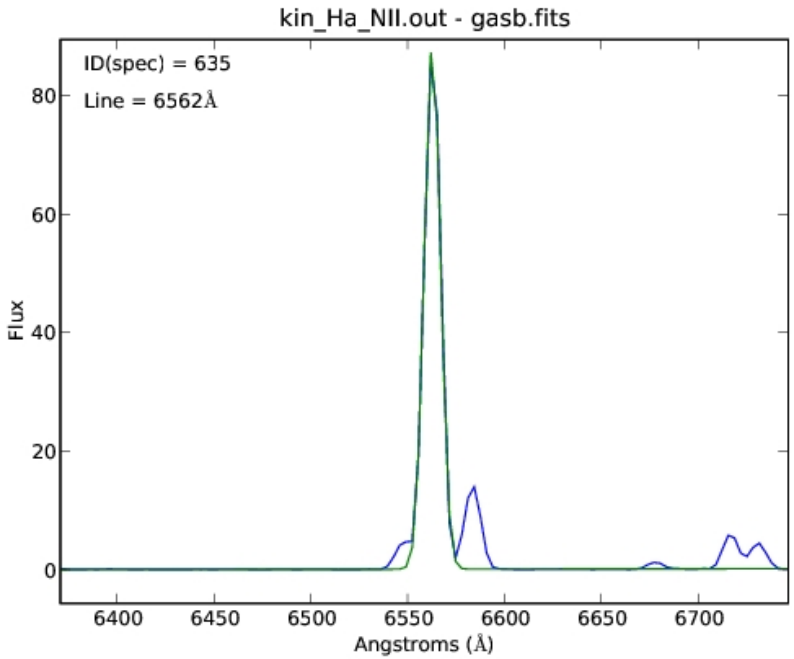
Similar results as combined Python + IRAF fitting tools



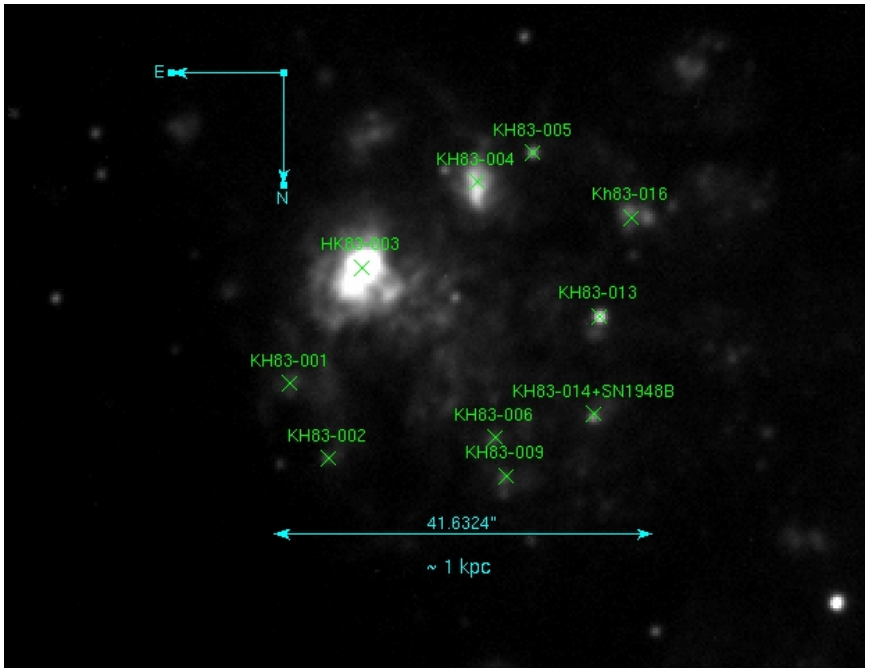
Fitting lines

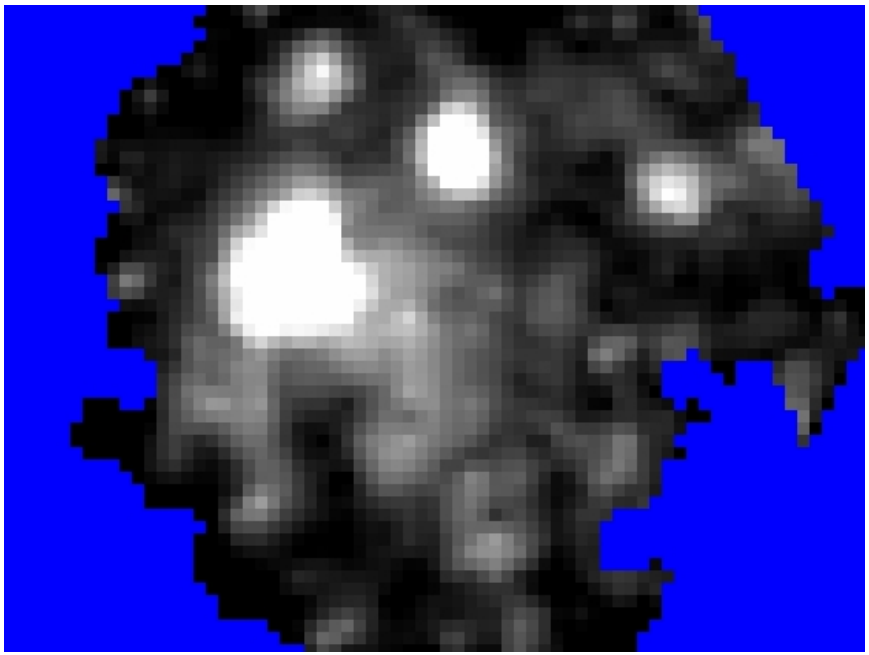
- Single Gaussian to each emission line
- Polynomial function to characterize continuum (low order)
- Definition of emission line systems (kinematically coupled) for debleding lines

Similar results as combined Python + IRAF fitting tools



Hα

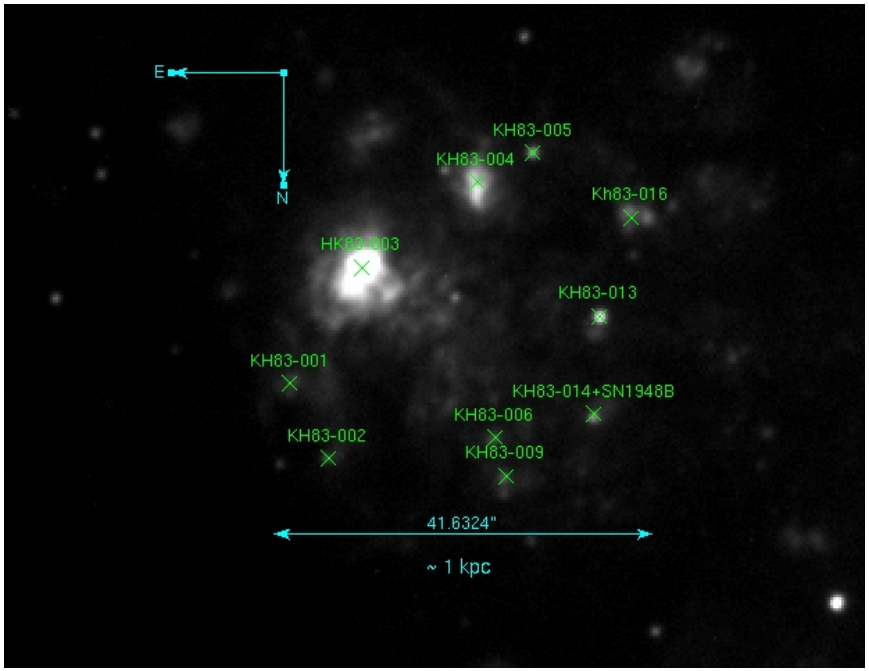


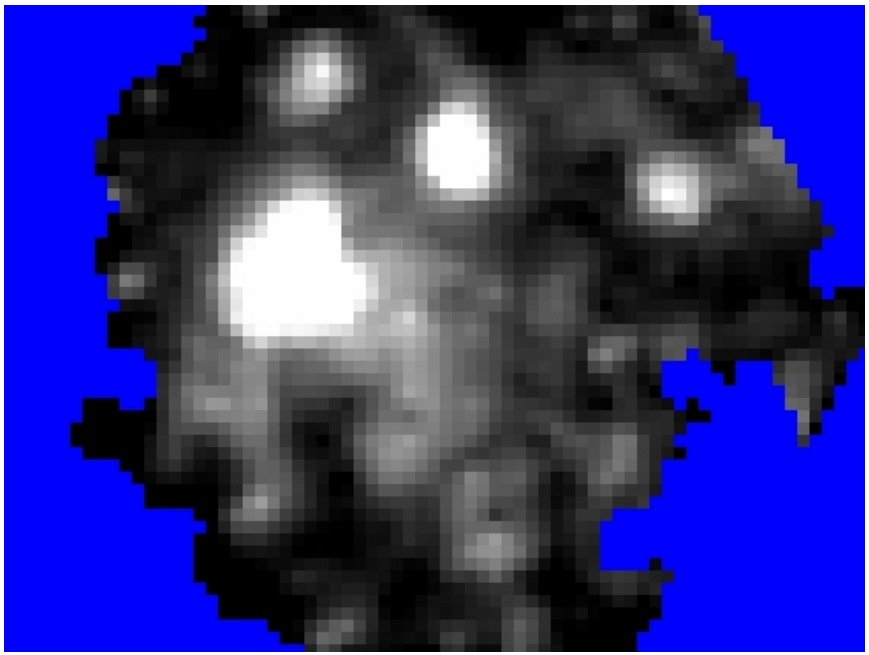


FINAL INTERPOLATION $\rightarrow$ 1 pixel $= 1'' \times 1''$

Mask spaxels: relative errors $\geq 30\,\%$

Hα

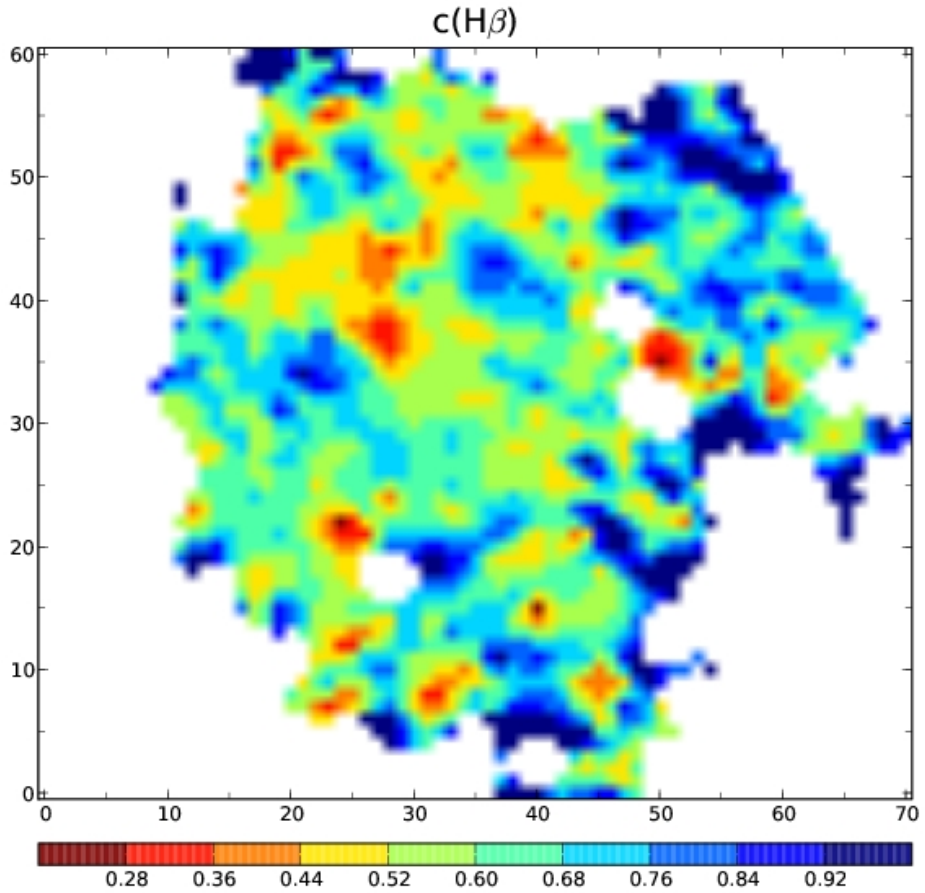




FINAL INTERPOLATION $\rightarrow$ 1 pixel $= 1'' \times 1''$

Mask spaxels: relative errors $\geq 30\,\%$

c(Hβ)

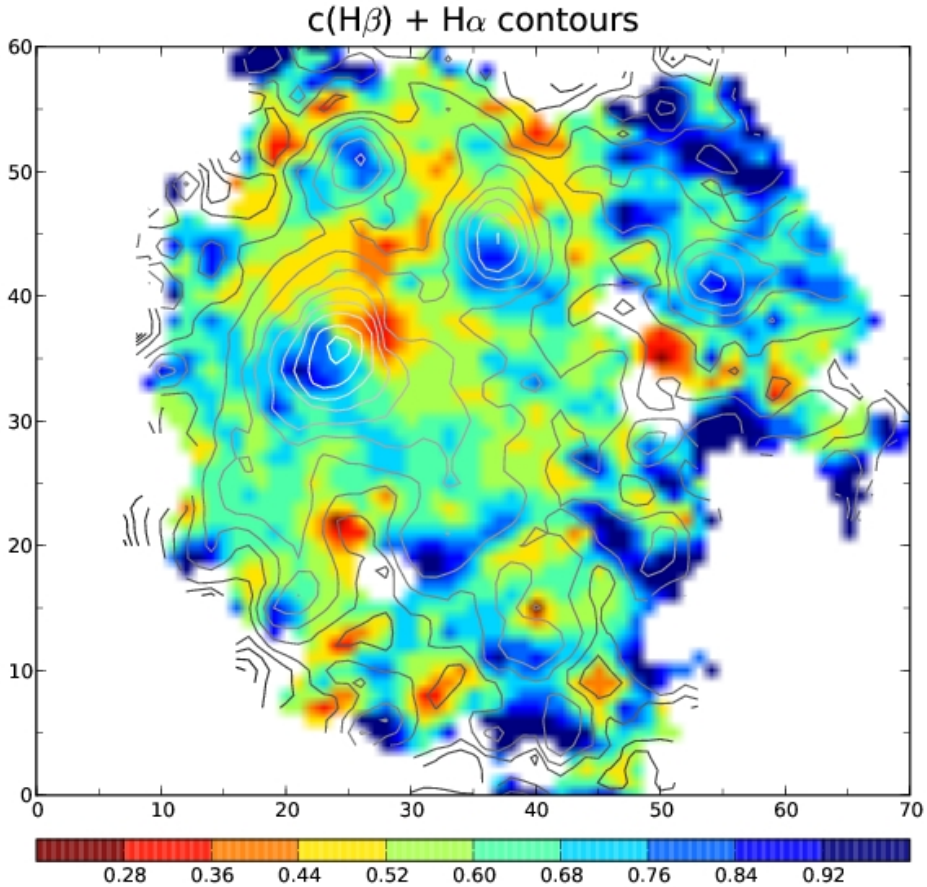


c(Hβ) calculation

- Reddening coefficient c(Hβ) for each fiber spectrum
- Balmer decrement derived from Hα/Hβ, compared to the theoretical value expected for case B recombination (Storey & Hummer, 1995)
- Cardelli et al. (1989) extinction law



c(Hβ)

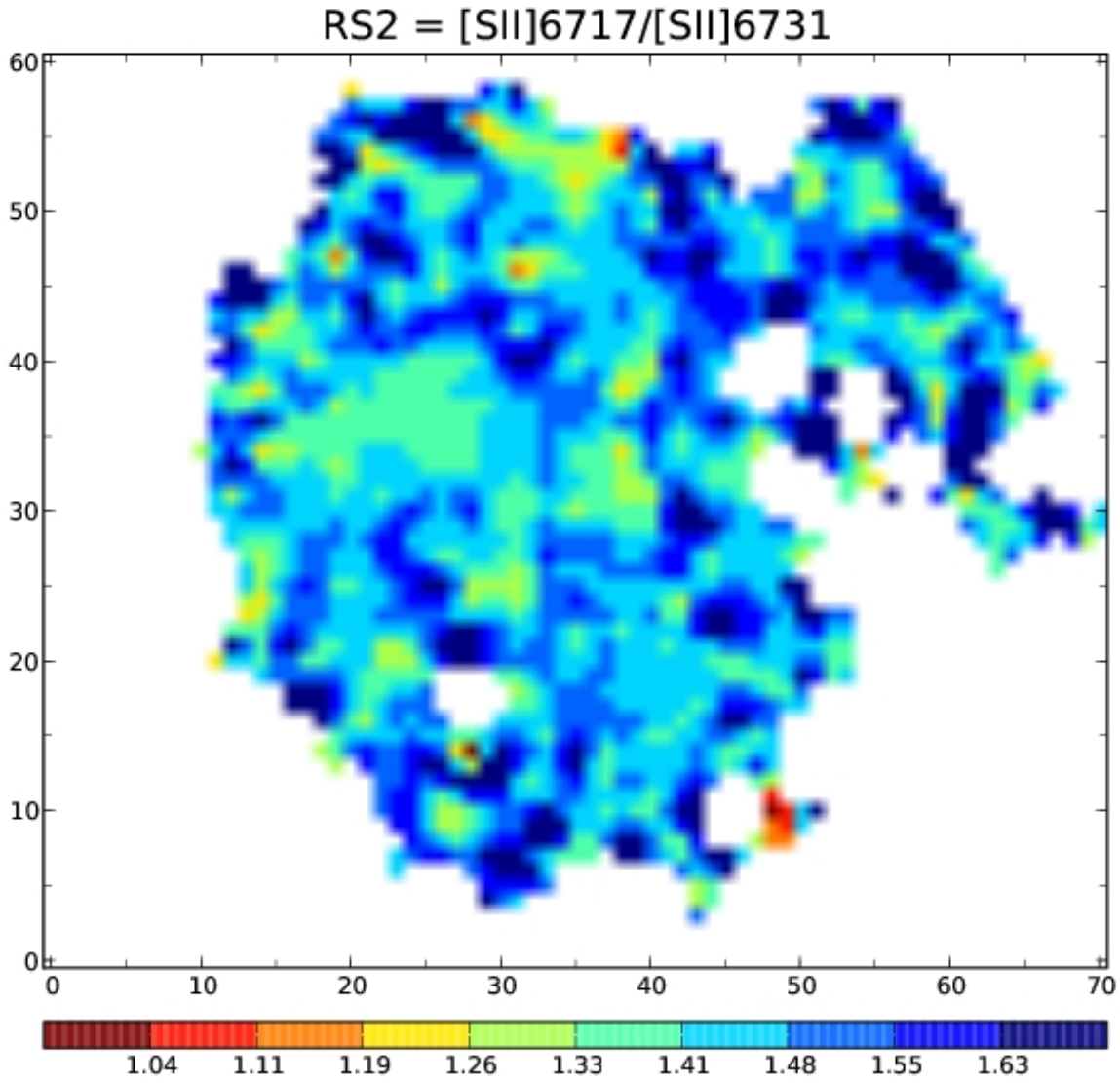


c(Hβ) calculation

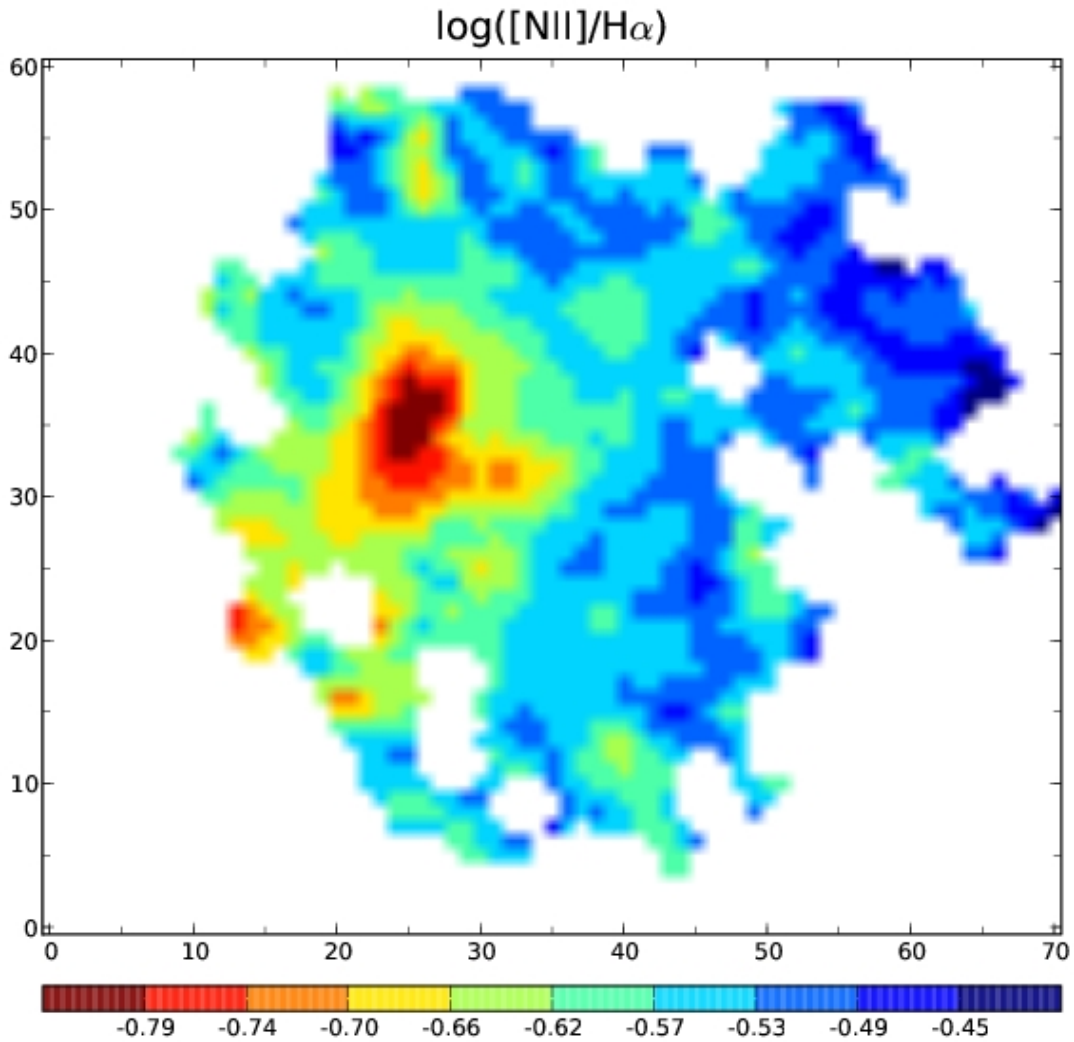
- Reddening coefficient c(Hβ) for each fiber spectrum
- Balmer decrement derived from Hα/Hβ, compared to the theoretical value expected for case B recombination (Storey & Hummer, 1995)
- Cardelli et al. (1989) extinction law



RS2: Density

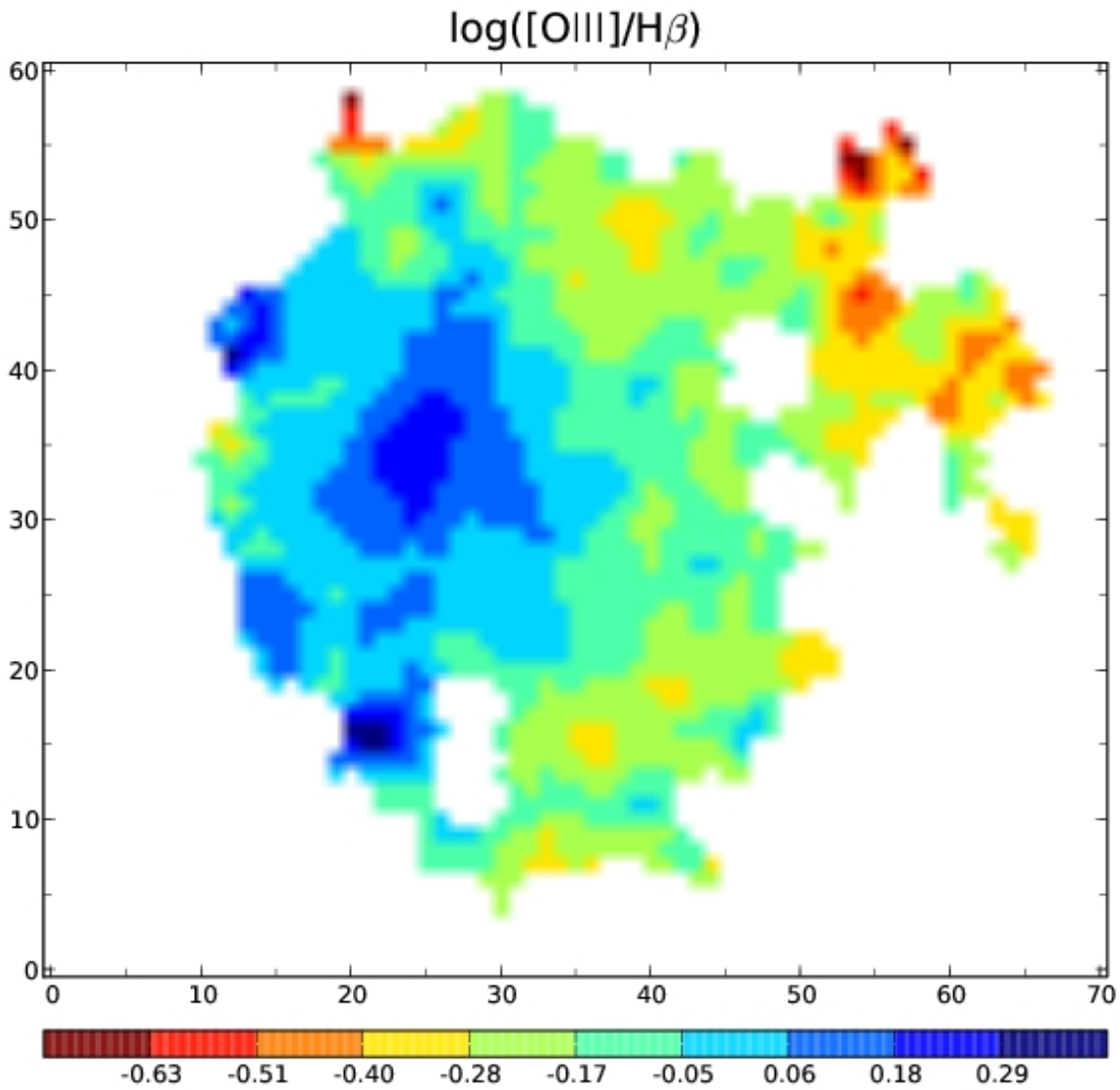

RS2 = [SII]6717/[SII]6731
60
50
40
30
20
10
0
0
10
20
30
40
50
60
70
1.04
1.11
1.19
1.26
1.33
1.41
1.48
1.55
1.63

[NII]/Hα

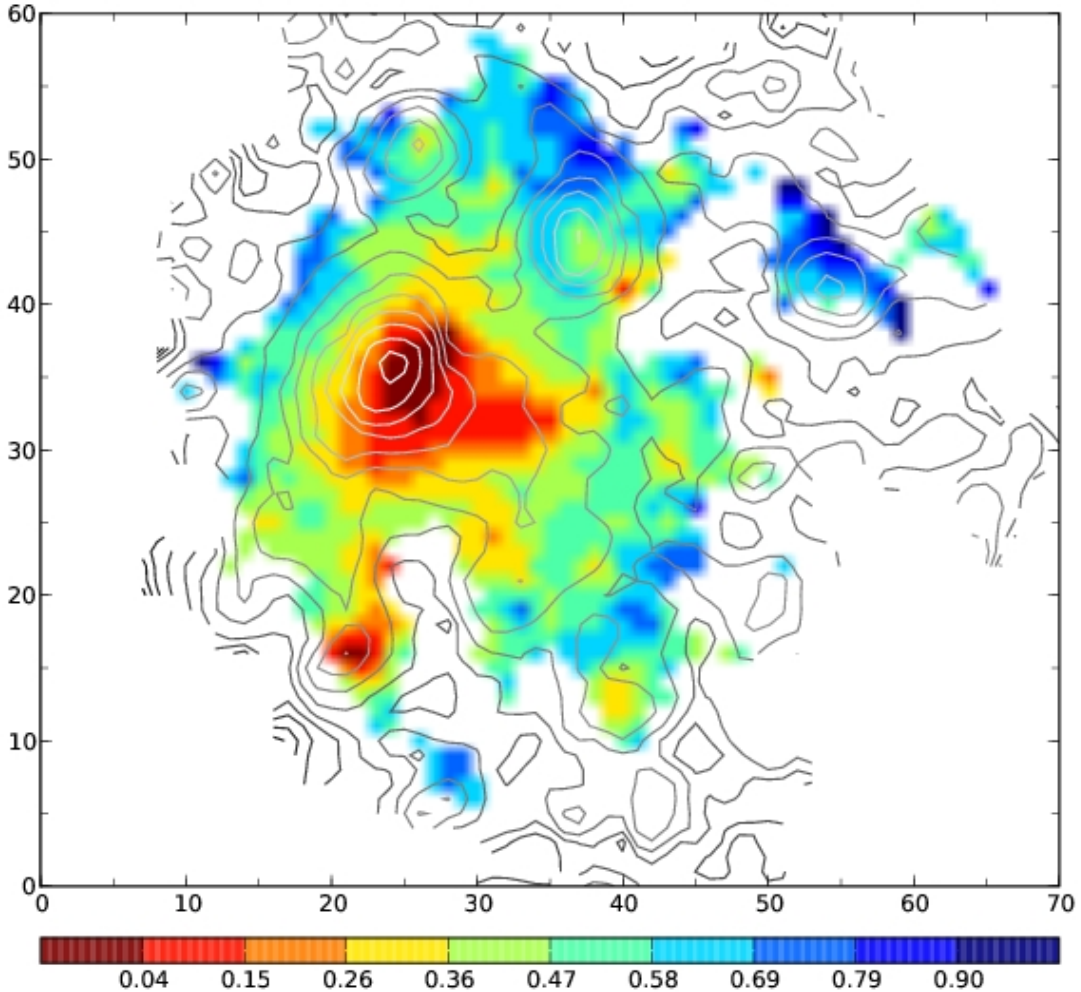


back

[OIII]/Hβ

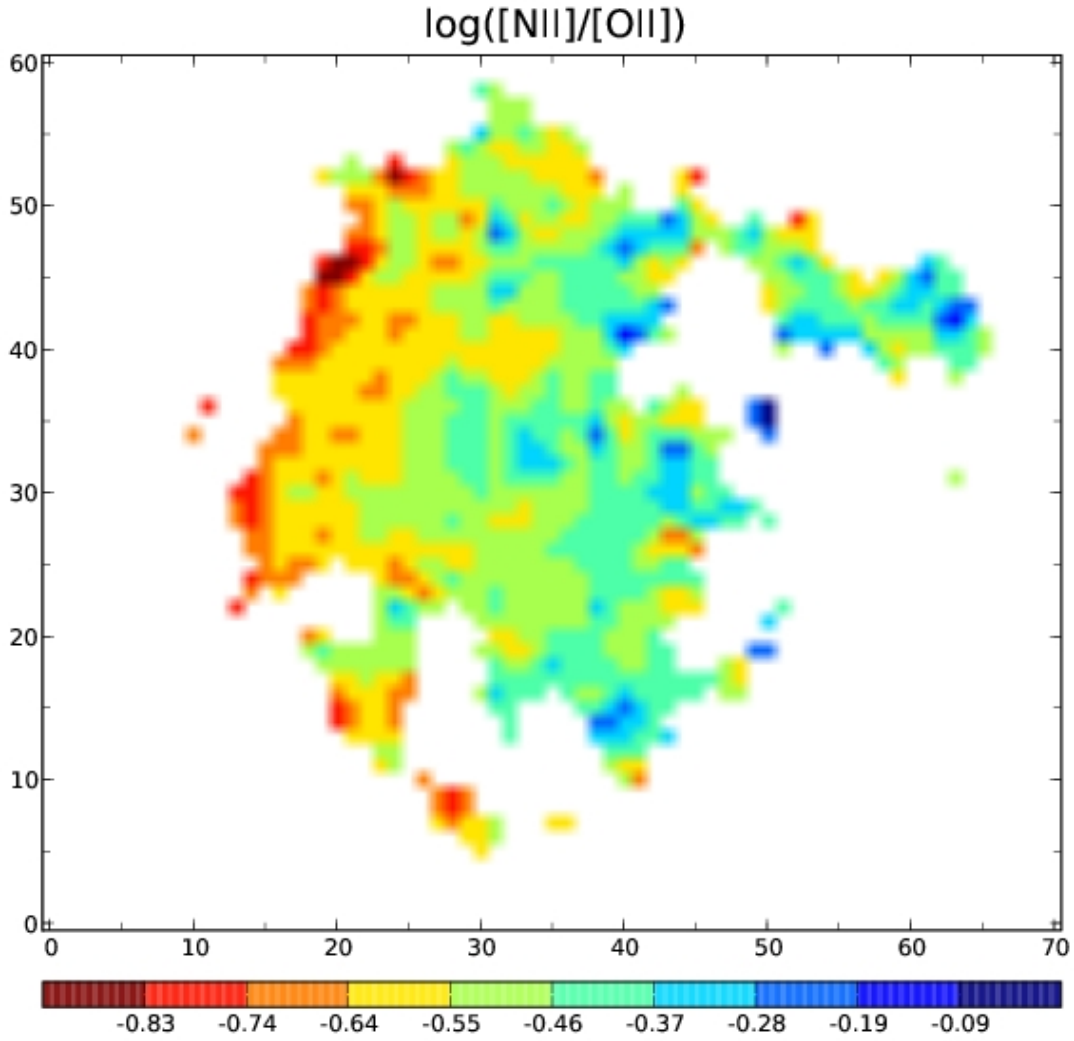

log([OIII]/Hβ)
60
50
40
30
20
10
0
0
10
20
30
40
50
60
70
-0.63
-0.51
-0.40
-0.28
-0.17
-0.05
0.06
0.18
0.29

[OII]/[OIII]



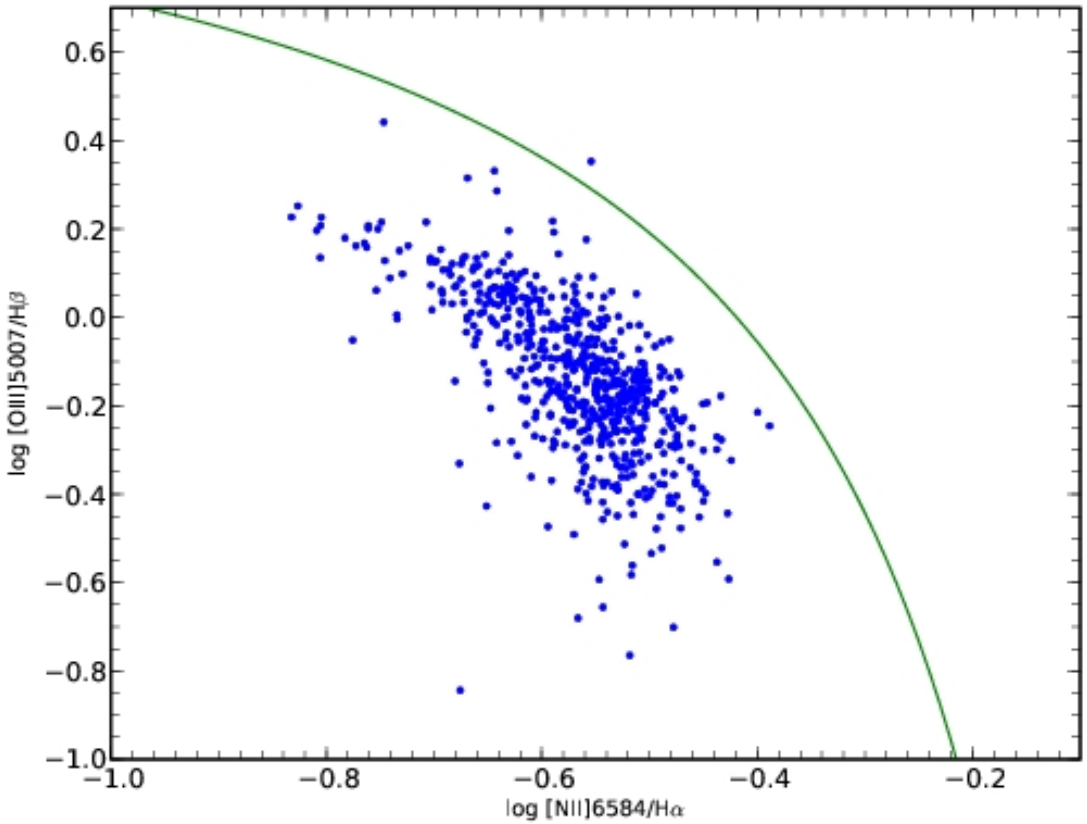
Hα contours

[NII]/[OII]

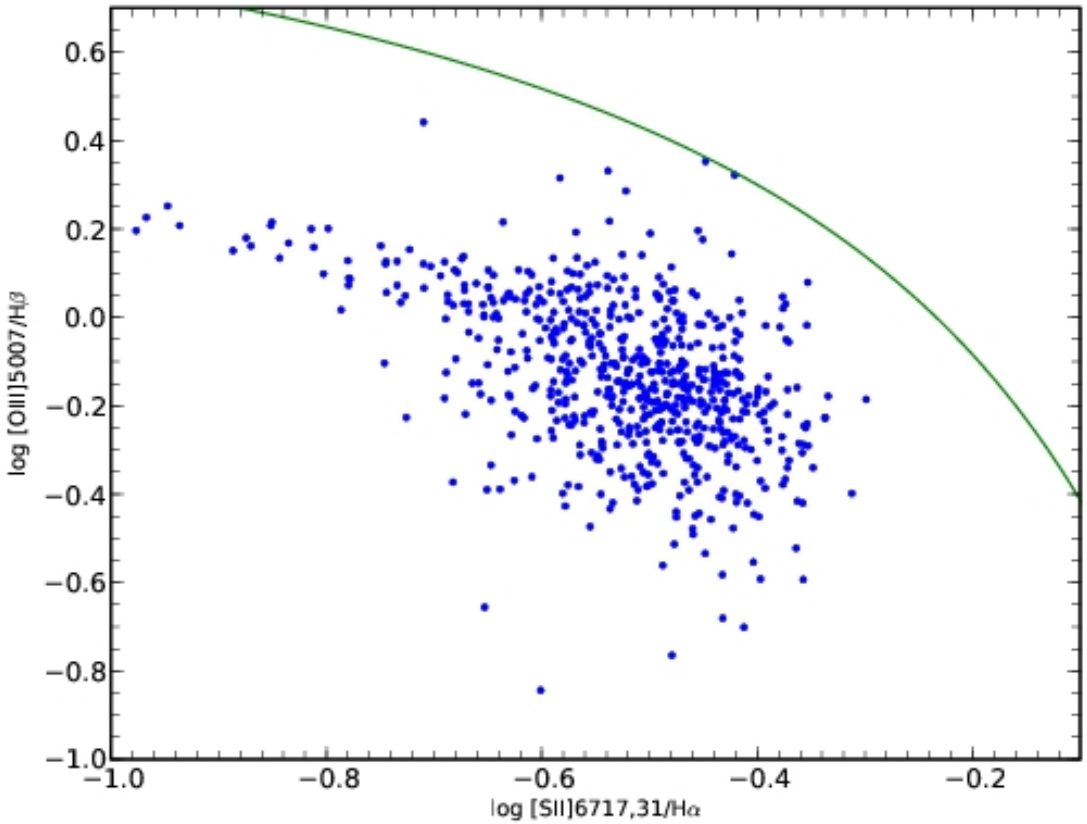

log([NII]/[OII])
60
50
40
30
20
10
0
0
10
20
30
40
50
60
70
-0.83
-0.74
-0.64
-0.55
-0.46
-0.37
-0.28
-0.19
-0.09

back

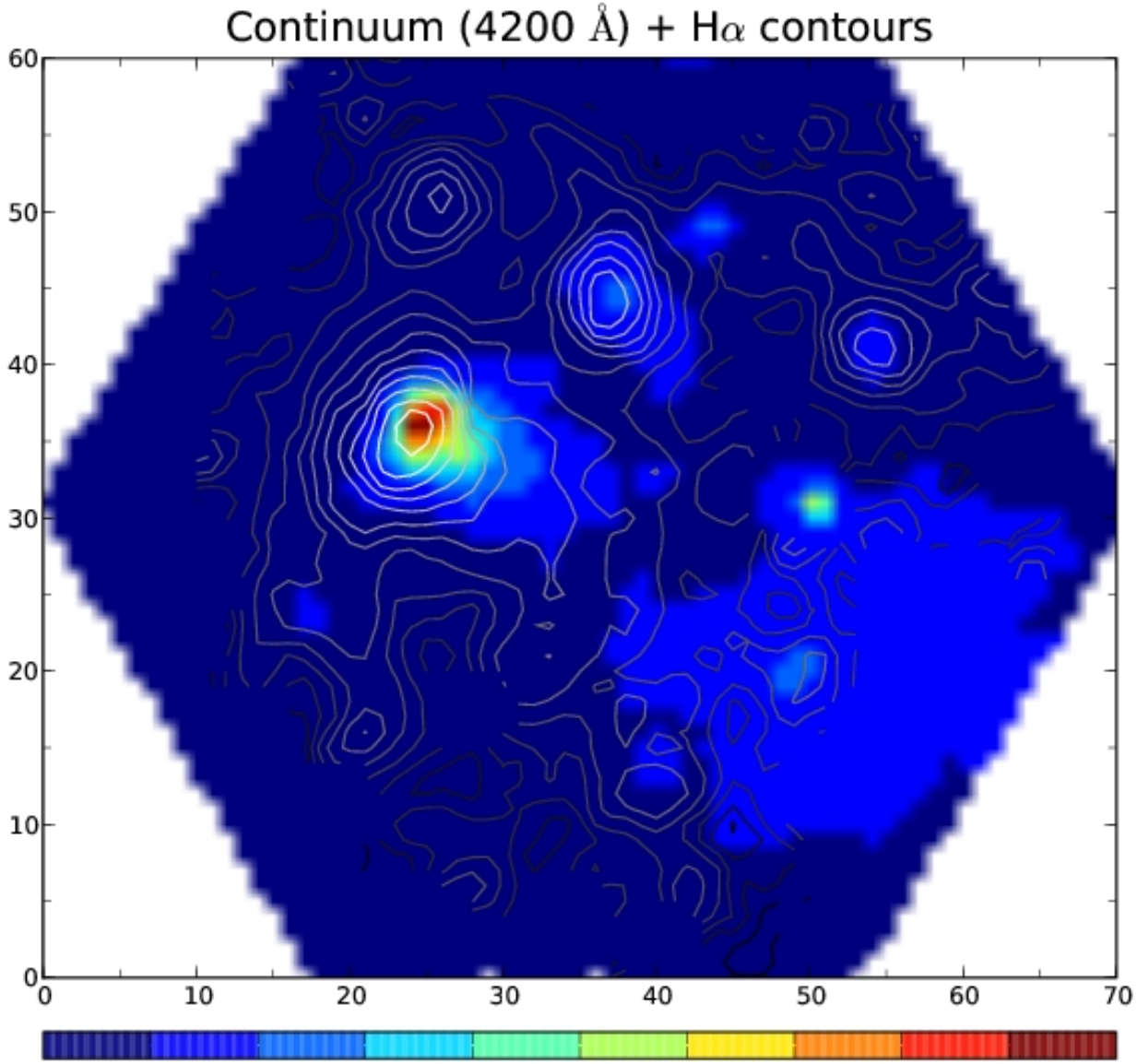
BPT Diagram: [NII]/Hα vs [OIII]/Hβ



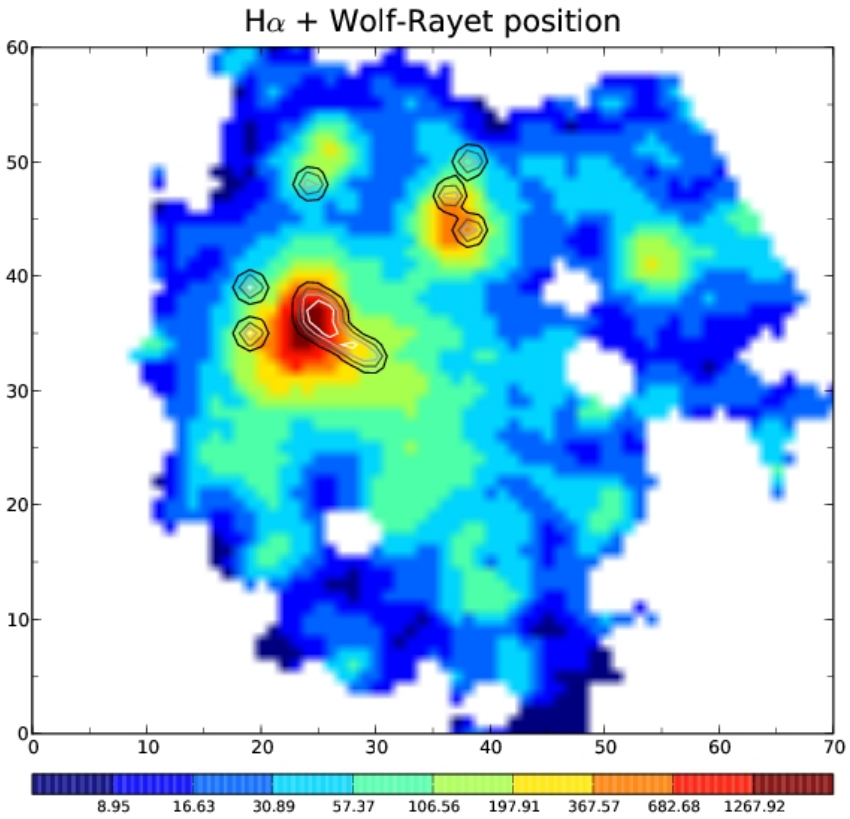
BPT Diagram: [SII]/Hα vs [OIII]/Hβ

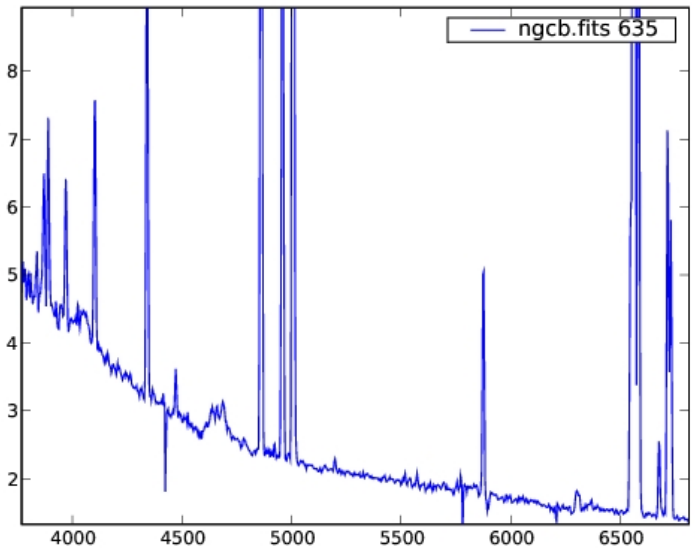


Blue Continuum

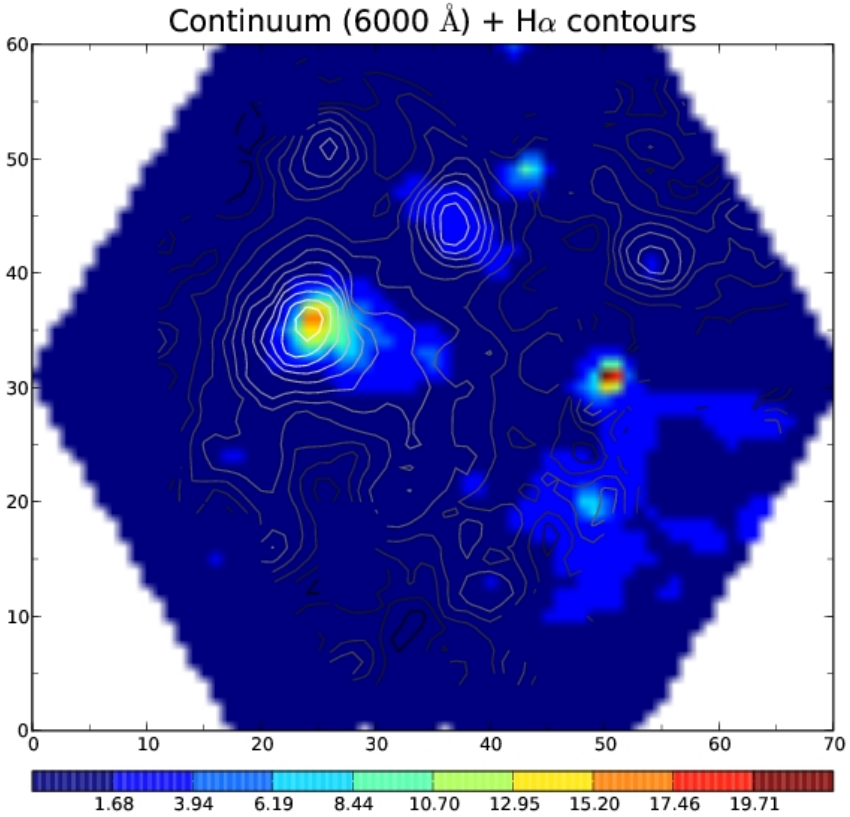


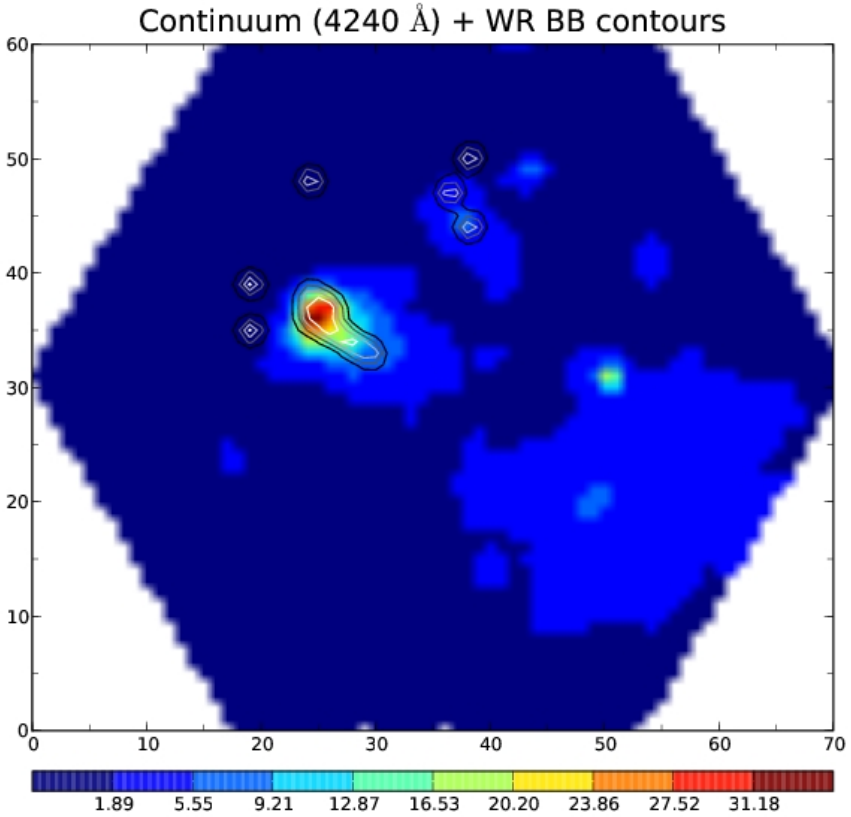
Wolf-Rayet Blue Bump



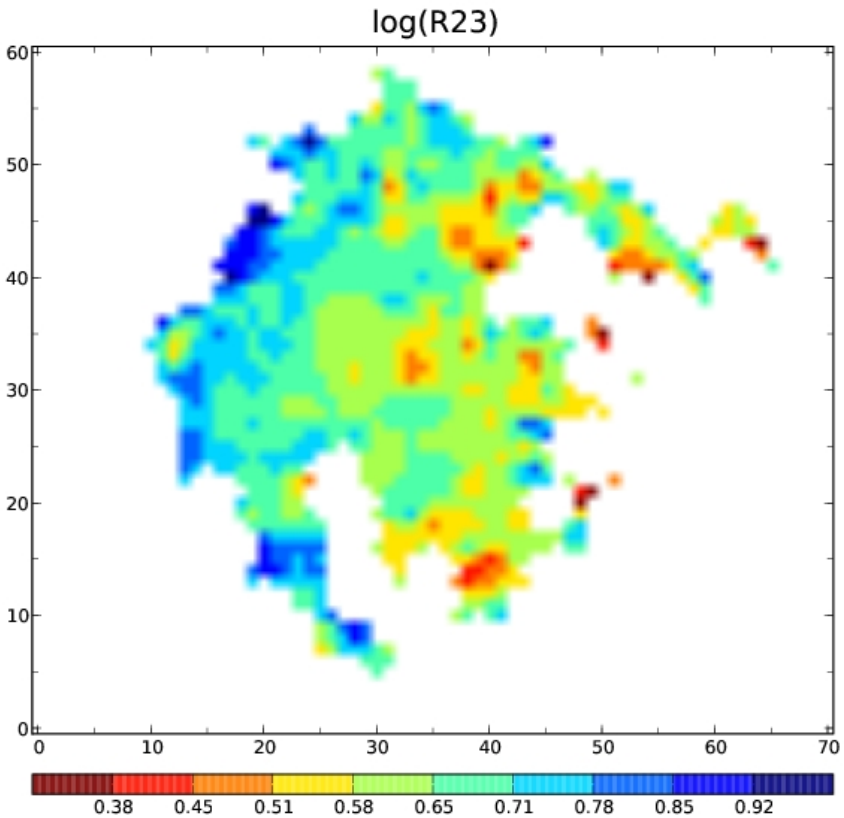


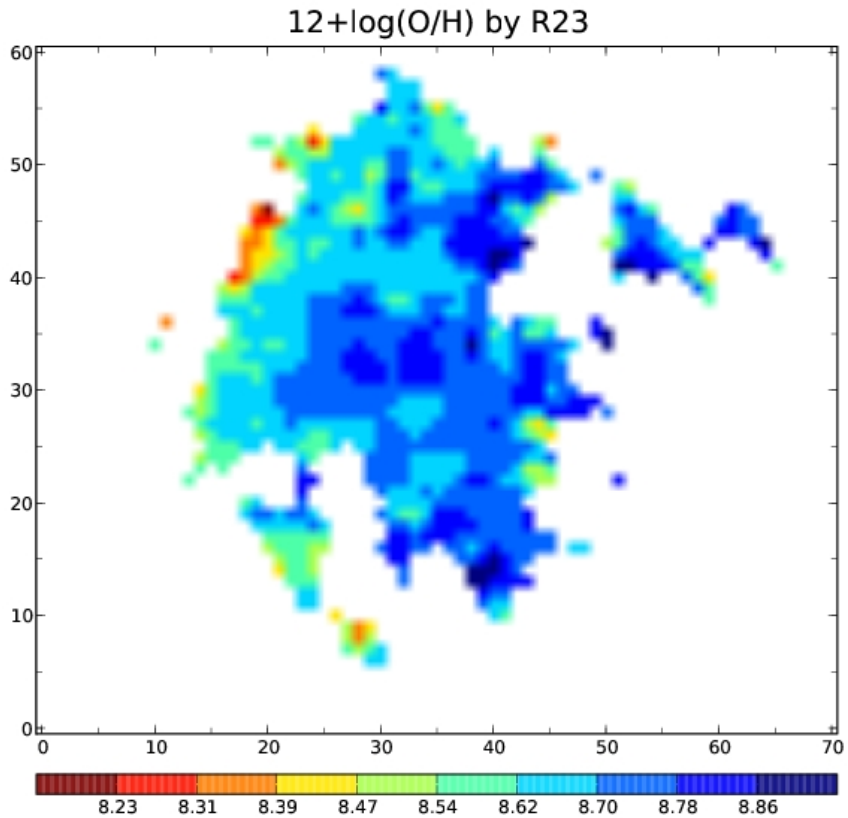
Wolf-Rayet BB and Continuum





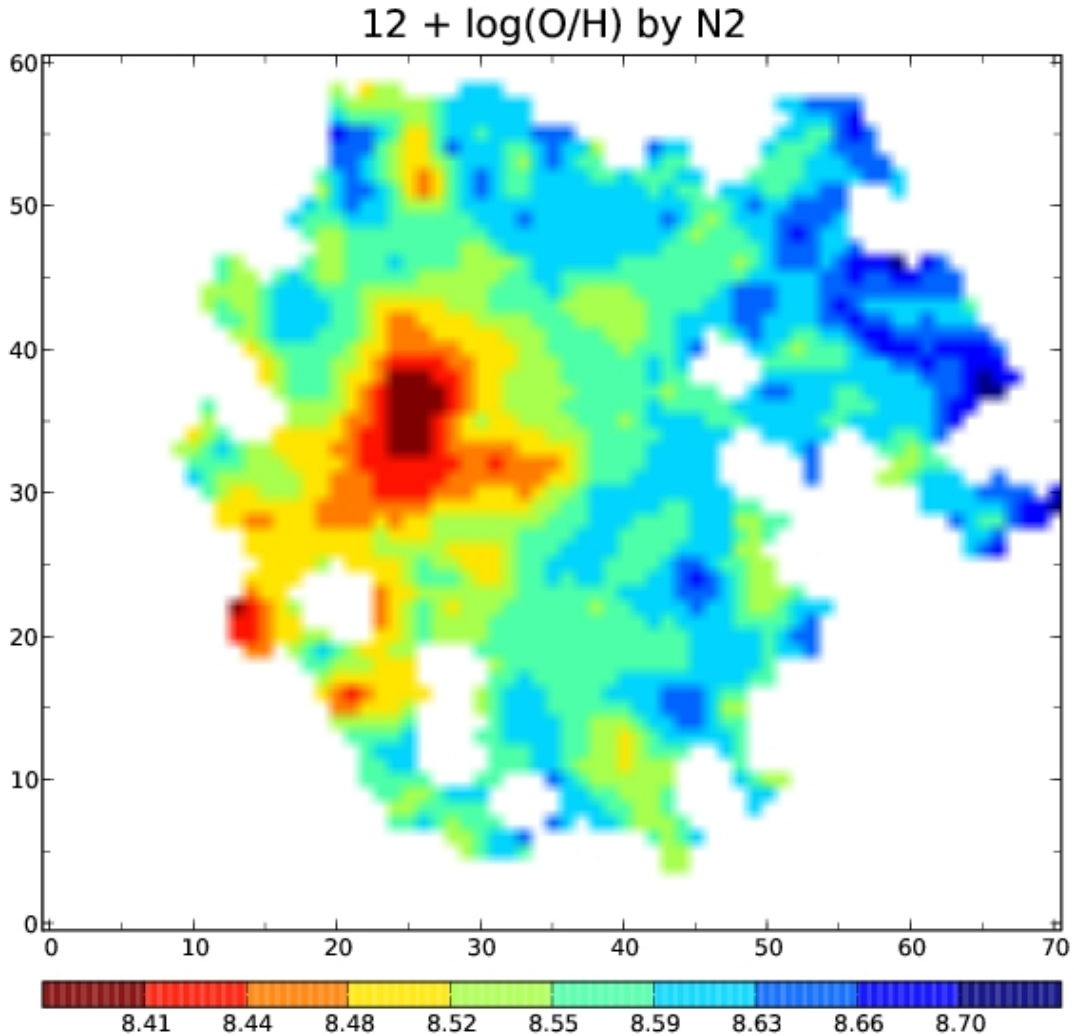
O23 = $(3727 + 4959 + 5007)/H\beta$ & O abundance





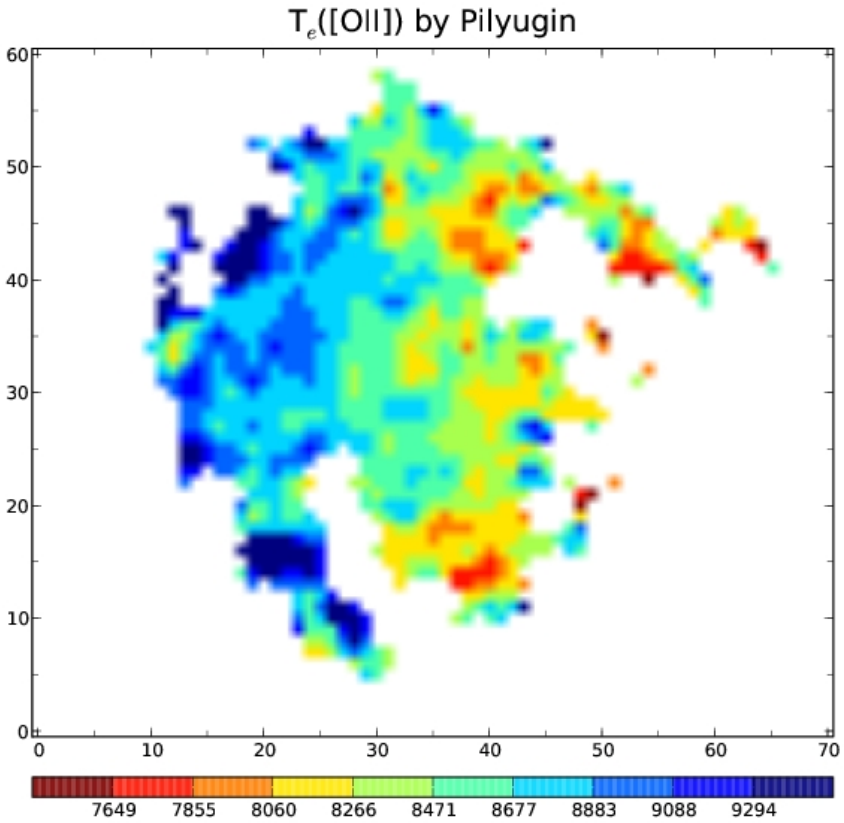
McGaugh (1991) with [NII]/[OII] to decide branch
log([NII]/[OII]) > -1.2 → UPPER branch here

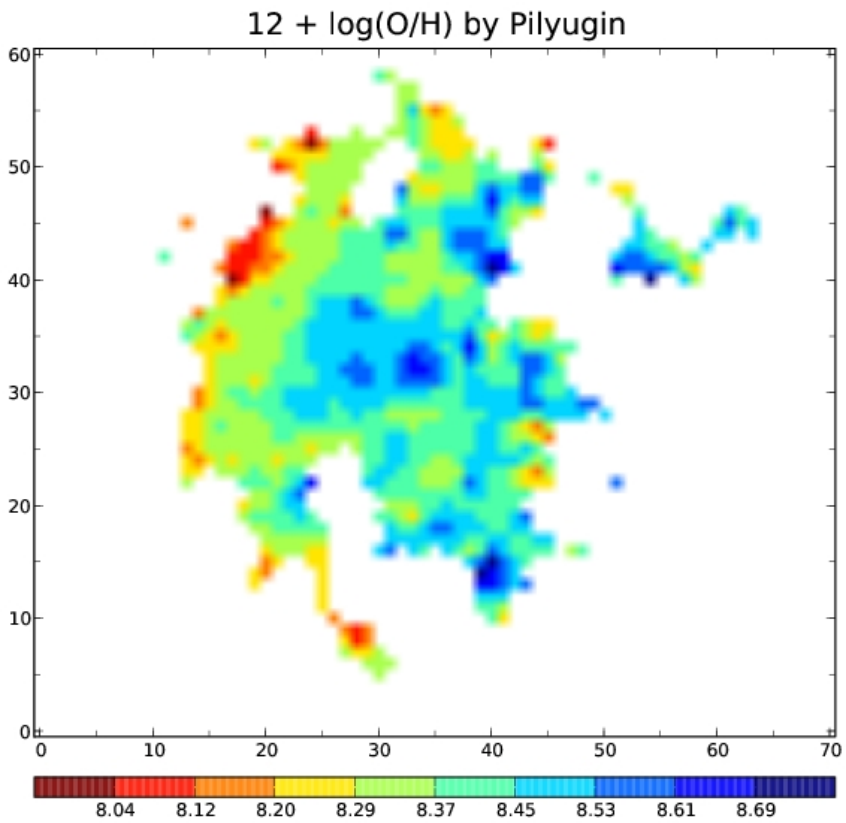
O abundance by N2 ([NII]/Hα)



here

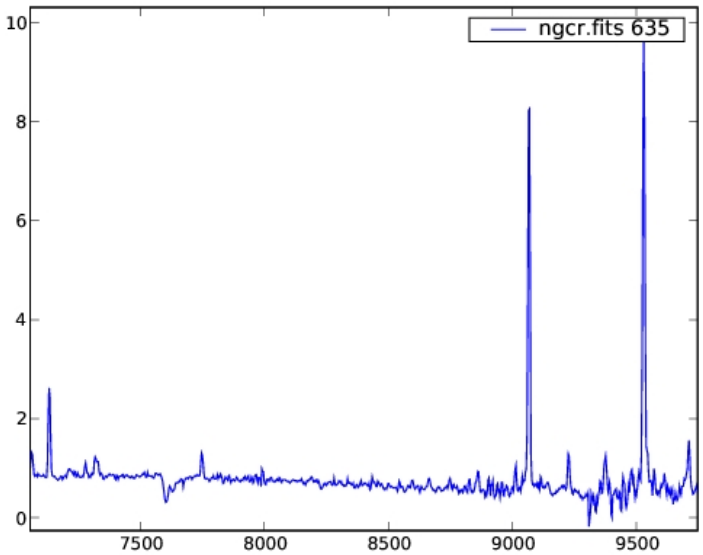
T([OII]) and O abundace by Pilyugin (2007)

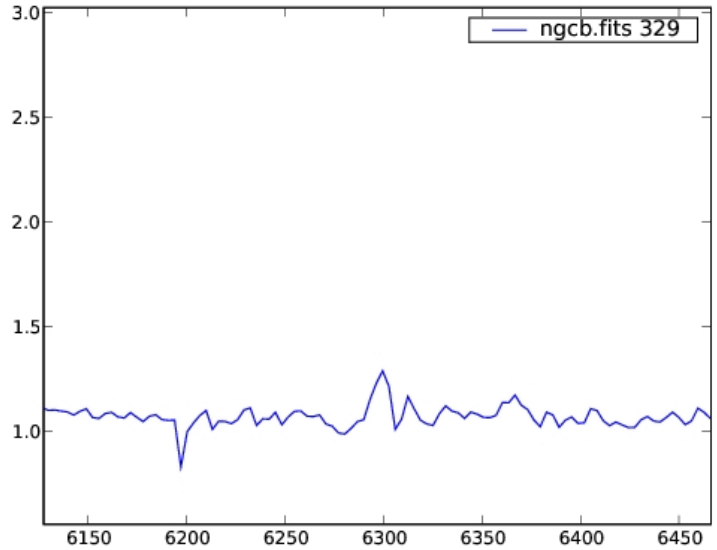




$$Q_{NII} = \frac{[NII]\lambda\lambda(6548, 6584)}{[NII]\lambda5755} = f\left(\frac{[OII]\lambda3727}{H\beta}; \frac{[OIII]\lambda\lambda(4959, 5007)}{[OII]\lambda3727 + [OIII]\lambda\lambda(4959, 5007)}\right)$$

Sulfur lines





Detected 6312 Å in 6 fibers $\longrightarrow$ T[SIII] $\sim$ 6600 $\pm$ 2000 ♦ 7600 $\pm$ 2000

Conclusions & Future Work

Conclusions

- Abundances from empirical calibrators in acordance with previous works
- Spectral features of WR stars detected clearly in several fibers
- Excitantion change considerably

Future work

- Compare direct measured temperature [SIII] 6312 (check flux calibration)
- Calculate number of WR stars
- Mocasin models with WR positions



Conclusions & Future Work

Conclusions

- Abundances from empirical calibrators in acordance with previous works
- Spectral features of WR stars detected clearly in several fibers
- Excitantion change considerably

Future work

- Compare direct measured temperature [SIII] 6312 (check flux calibration)
- Calculate number of WR stars
- Mocasin models with WR positions



Conclusions & Future Work

Conclusions

- Abundances from empirical calibrators in acordance with previous works
- Spectral features of WR stars detected clearly in several fibers
- Excitantion change considerably

Future work

- Compare direct measured temperature [SIII] 6312 (check flux calibration)
- Calculate number of WR stars
- Mocasin models with WR positions



THANKS!

